# Interference effects on bound-to-continuum quantum dot absorption

J. Houel,[1] S. Sauvage,[1,a)] A. Lemaître,[2] and P. Boucaud[1,b)]
[1]*Institut d'Electronique Fondamentale, CNRS–Univ Paris-Sud 11, Bâtiment 220, 91405 Orsay, France*
[2]*Laboratoire de Photonique et de Nanostructures, CNRS, Route de Nozay, 91460 Marcoussis, France*

(Received 12 January 2010; accepted 10 March 2010; published online 19 April 2010)

We have investigated the bound-to-continuum absorption of InGaAs quantum dots as a function of *n*-doping. We show that the combination of multipass waveguide geometry, large number of quantum dot layers, and spectrally broad absorption leads to significant spectral oscillations on the absorption spectra. The oscillations result from the standing wave pattern caused by the interference of optical beams incident and totally reflected at the sample/air interface. The spectral modulations on the absorption spectra should not be attributed to resonant intersublevel transitions. © *2010 American Institute of Physics*. [doi:10.1063/1.3385313]

## I. INTRODUCTION

The study of quantum dot intersublevel transitions has recently attracted a wide interest. Intersublevel transitions between states of the conduction band either bound-to-continuum transitions[1,2] or bound-to-bound transitions[3–5] can bring valuable information for quantum dot spectroscopy. Intersublevel transitions can also be used to develop quantum dot infrared phototodetectors and numerous studies have been reported in this field.[6–10]

One difficulty in the study of quantum dot absorption is the precise assignment of the optical transitions from the transmission spectra. The transition between the ground state and the first excited state, usually denoted as S-P transition, can be easily observed at low or room temperature in transmission measurements at normal incidence since this transition is in-plane polarized. The situation is different for bound-to-continuum transitions which are mainly polarized along the *z*-growth axis[11] and thus require the use of a multipass geometry to investigate the polarization dependence of the absorption and to couple light with an electric field along the growth axis.[1,12] Another advantage of the multipass geometry is to allow an increase in the absorption amplitude as compared to a single pass. In principle, this type of measurement is not an issue and it has been widely used to study quantum well intersubband transitions. As compared to quantum wells, the study of InGaAs/GaAs quantum dots in the mid-infrared presents however some specificities. As the quantum dot density is relatively small, i.e., $4\times10^{10}$ cm$^{-2}$ for standard growth conditions, the absorption of a single layer is quite small. This problem can be circumvented by growing a large number of quantum dot layers (80 for example) resulting in a large active total thickness. The second specificity is the large broadening of the bound-to-continuum transitions which can be larger than 150 meV. As intersublevel absorption is spanned over a large spectral range, the observation of interference effects is more likely to occur. The role of interferences can become detrimental since they can mask tiny features that should be observed on the absorption spectra.[13–15] Among these tiny features is the transition from S to "D" levels, as defined in Ref. 16. These transitions have been theoretically predicted to occur around 100–120 meV using a eight band $\mathbf{k}\cdot\mathbf{p}$ formalism for the three-dimensional solution of the Schrödinger equation.[17] This transition has been experimentally evidenced by resonant second harmonic generation experiments[18] or single dot absorption spectroscopy.[16,19] Its direct observation in absorption measurements on quantum dot ensembles is more difficult, although it has been claimed to be observed in Refs. 20 and 21.

In this work, we have investigated the spectral dependence of the bound-to-continuum absorption in InGaAs quantum dots as a function of the doping. This study allows to distinguish the features associated with the bound-to-continuum absorption and those associated with interference effects in the multilayers. The interference effects resulting from the standing wave pattern due to total internal reflection are evidenced through their dependence as a function of the incident angle in the multipass geometry. These measurements allow to better understand the mid-infrared spectroscopy of quantum dots.

## II. SAMPLES AND EXPERIMENTAL SET-UP

The studied self-assembled InGaAs quantum dot samples were grown by molecular beam epitaxy on semi-insulating GaAs substrates by depositing pure InAs on GaAs. They consist of 80 InGaAs quantum dot layers separated by 50 nm thick GaAs spacer layers. The total thickness of the active structure is thus 4 $\mu$m. The quantum dots are modulation-doped using a silicon delta doping 2 nm beneath the InGaAs layer. The dot density $n_0$ is $4\times10^{10}$ cm$^{-2}$. The nominal doping is varied between 0.5 carrier per dot and 3 carriers per dot on average. For infrared spectroscopy, the absorption of the samples is either probed at normal incidence or using a multipass waveguide with polished facets at 45°. The number of total internal reflections at the quantum dot active region/interface is 10. The measurements presented below are performed at room temperature with a Fourier transform infrared spectrometer. We have also performed

a)Electronic mail: sebastien.sauvage@ief.u-psud.fr
b)Electronic mail: philippe.boucaud@ief.u-psud.fr. http://pages.ief.u-psud.fr/QDgroup/index.html.

 

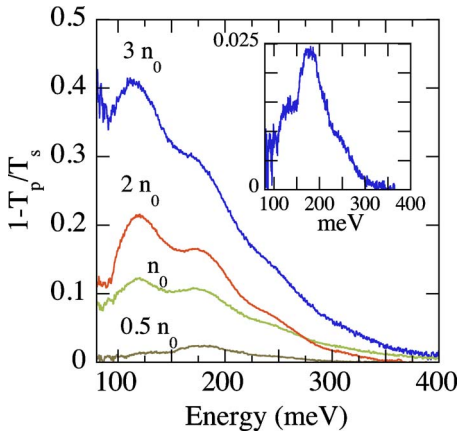


FIG. 1. (Color online) Absorption spectra measured in a multipass geometry as given by $1-T_p/T_s$ for InGaAs quantum dot samples with different nominal dopings. $T_{p(s)}$ is the transmission in $p(s)$ polarization. The transmissions are normalized by the transmission measured for the same polarization with a reference GaAs sample containing undoped quantum dot layers. The measurements are performed at room temperature. The inset shows a zoom on the spectrum of the lightly doped sample (0.5 $n_0$).

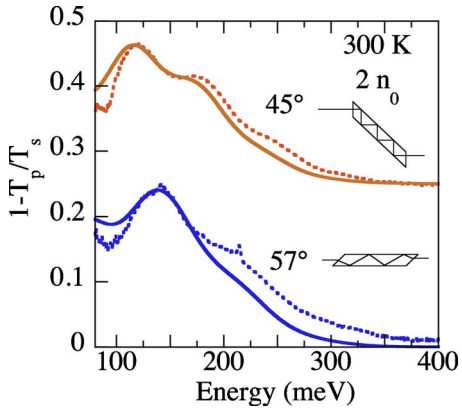


FIG. 2. (Color online) Absorption spectra in multipass geometry of the quantum dot sample nominally doped at 2 $n_0$ as a function of the incident angle on the quantum dot layers (dashed lines). The full lines correspond to the modeling which accounts for the standing wave effect. The insets show schematics of the sample orientation used for measurements.

experiments at low temperature to probe the S-P optical transition. The transmission measurements are performed in *s* and *p* polarizations. *s* polarization corresponds to an electric field polarized in the quantum dot layer plane while the *p* polarization has electric field components along the *z*-growth axis and in the layer plane. Each transmission spectrum is normalized by the transmission recorded for the same incident polarization with a reference multipass sample with undoped quantum dots. The spectra presented below correspond to the ratio of transmission in *p* polarization ($T_p$) divided by the transmission in *s* polarization ($T_s$). This ratio allows to highlight the contribution of the quantum dot absorption polarized along the growth axis. It partly removes the contribution of free carrier absorption which starts to be significant below 150 meV for the doped samples with 3 $n_0$.

## III. RESULTS

Figure 1 shows the dependence of $1-T_p/T_s$ at room temperature for different nominal dopings. The inset in Fig. 1 shows a zoom on the absorption spectrum of the sample doped at 0.5 $n_0$. The maximum of absorption is observed at 180 meV and corresponds to the bound-to-continuum absorption from the ground state.[1] A small shoulder can be observed at 120 meV as well as another one at 240 meV. These shoulders are more clearly evidenced for samples with higher dopings because of the better signal to noise ratio and the increased broadening of the transitions. For the sample doped at $n_0$, the resonance around 120 meV starts to dominate the absorption spectrum, the resonance at 180 meV is still present while the shoulder at 240 meV is more clearly evidenced. The same trend continues as we increase the nominal doping and the resonance at 120 meV becomes even more pronounced on the spectra. Since different resonances are present, the assignment of the quantum dot optical transitions is not straightforward as different optical transitions might contribute. The *z* polarized transition from the S ground state to the wetting layer states and GaAs continuum is the most obvious candidate. Transitions from the S state to the D states could also contribute as they are expected to occur around 100–120 meV.[16] A small contribution to the absorption from the excited states can also exist even if, with a 3 $n_0$ nominal doping, the quantum dots are only partly filled at room temperature. This feature is a consequence of the thermal emission which reduces the absorption amplitude by a factor of 3–4 between low temperature and room temperature.[5] Measurements performed at room temperature and normal incidence on the same samples show that, as the doping increases, the inhomogeneous broadening of the S-P transition increases. We also observe a small redshift of the S-P transition as the doping increases. This redshift and broadening increase are a consequence of the quantum dot occupancy and Coulomb effects within the quantum dots.[22,23]

Figure 2 shows a comparison of the absorption spectra measured for an incident angle on the facet of 0° (i.e., 45° inside the material) and an incident angle on the coupling facet of 45° obtained by rotating the sample (i.e., 57° inside the material measured from the normal of the quantum dot planes). The striking feature is the strong blue-shift by more than 20 meV of the resonances as the incidence of light is modified.

## IV. MODELING OF INTERFERENCES

Several features might contribute to the interferences. As the 4 $\mu$m quantum dot stacking is doped, it is characterized in the investigated spectral range by a lower real value of refractive index of refraction as compared to the semi-insulating GaAs substrate (resistivity $>10^7$ $\Omega$ cm). This change of refractive index gives rise to different reflection coefficients in *s* and *p* polarizations between the 4 $\mu$m thick doped layer and the GaAs substrate and might lead to oscillations in the transmission spectra. This effect has been previously evidenced in absorption spectra of quantum dots embedded between heavily doped layers used for contacts.[8,24] We have modeled this effect using a transfer matrix method. However, it turns out that this effect cannot explain the experimentally observed features. In such model, the oscilla-

tions are only significant in *s* polarization. In *p* polarization, there is almost no oscillation in the transmission spectra since the incident angle is very close to the Brewster angle inside the material and hardly no reflection occurs at the interface between the doped and undoped layers. Experimentally, modulations on the transmission spectra are observed in *p* polarization but not in *s* polarization. The change of refractive index between the layers, which would have a significant impact with highly doped structures, cannot explain the presently observed oscillations. The origin of the oscillations is the following. In the total reflection geometry, a standing wave pattern developes because of the interference of the incident and reflected waves at the sample/air interface. The total reflection leads to a significant phase shift (around 150° for an incident angle of 45°). This phase shift is at the origin of the quasinode of the electric field along the *z*-growth axis close to the GaAs/air interface and consequently leads to a vanishing *z* polarized absorption for a layer close to the surface. This effect was pointed out in the study of quantum well intersubband transitions.[25] The formation of standing wave patterns close to the surface was widely discussed in the framework of quantum well intersubband absorption measurements[26,27] and also in order to describe the performances of quantum well infrared photodetectors.[28] It results in a spatial modulation of the electric field along the *z*-growth axis with a periodicity which depends on the wavelength and consequently leads to an effective renormalization of the absorption amplitude. This effect becomes significant for the quantum dot samples as the absorption has to be integrated over a thickness which is of the order of the wavelength in the material ($\lambda/n$). Meanwhile, we are looking at broad transitions and consequently investigate a large spectral range, a case which differs from the one usually encountered with quantum wells. According to Ref. 26, the spatial modulation of the light intensity polarized along the *z*-growth axis is given by

$$I_z \propto 2\sin^2(\alpha)[1+\cos(2k_z z-\delta_{\parallel})], \tag{1}$$

$$\delta_{\parallel}=2\arctan\left(\frac{n\sqrt{n\sin^2(\alpha)-1}}{\cos(\alpha)}\right), \tag{2}$$

where $k_z=2\pi n\cos(\alpha)/\lambda$, $n$ is the refractive index, $\alpha$ the incident angle at the interface, and $\delta_{\parallel}$ the phase change at the total reflection for *p* polarized light. To obtain the quantum dot absorption, one has to integrate this standing wave pattern intensity over the 4 $\mu$m thick quantum dot layer as the absorption depends on the local amplitude of the square of the electric field. The effect of this intensity distribution is illustrated in Fig. 3 where the spatial intensity profile at 100 meV is shown in the inset. The bottom curve of Fig. 3 shows the modulation of a Gaussian-broadened absorption centered at 180 meV, corresponding to the situation for the sample doped with 0.5 $n_0$. The Gaussian absorption corresponds roughly to the bound-to-continuum quantum dot absorption even if it does not account for the asymmetry of the absorption profile. One observes shoulders around 120 and 240 meV as in the experiments, indicating that these modulations are a direct consequence of the interference patterns. If the Gaussian maximum is shifted to lower energy, the resonance around 120 meV can become even more pronounced. This effect is also shown in Fig. 3 (top) for a Gaussian centered at 125 meV. This situation corresponds to the case of the more heavily doped sample. This shift of the bound-to-continuum transition is a consequence of the change in the quantum dot population distribution and Coulomb effects as observed on the S-P transition. In the calculation, the value of 125 meV was chosen in order to reproduce the respective amplitudes of the resonances at 120 and 180 meV. If a baseline is subtracted from the experimental data, the respective amplitudes of these resonances can be modified, leading to a change in the energy value of the bound-to-continuum resonance. Because of this baseline, the amplitude of the Gaussian absorption was also adjusted in order to fit the experimental amplitude. In the modeling, the incident angle was set to 47°, a value slightly different from the nominal one since it provides a better agreement. This change of 2° reflects the uncertainties of the experimental measurements. As seen in Fig. 3, the regularly spaced oscillations on the spectra (~60 meV) are a consequence of the quantum dot layer thickness. Clearly, the resonance around 120 meV is not a signature of bound-to-bound S-D intersublevel transitions. The energy shift of the resonances coming from the change of the incident angle is illustrated in Fig. 2 through the full lines which correspond to the modeling for two distinct incident angles. As seen, the standing wave effect explains the dependence of the absorption shape as a function of the angle. The change in the incident angle results in a 20 meV shift of the resonances as observed experimentally. The key features resulting from this modeling are the following: the only transition which contributes to the absorption is the bound-to-continuum transition. The origin of the additional features which can be observed on the spectra is associated with interference effects which are more easily evidenced when absorption is broad. They are not associated with bound-to-bound transitions. Features associated with bound-

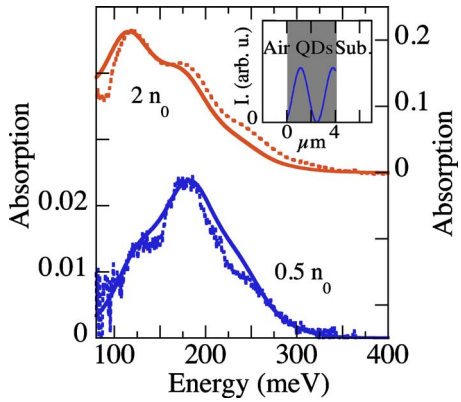


FIG. 3. (Color online) Comparison between the modeling of the absorption spectra taking into account the interference effects due to the standing waves (full lines) and the experimental measurements (dashed lines). (a) The bottom curve takes into account a Gaussian absorption centered at 180 meV corresponding to the quantum dot sample doped at 0.5 $n_0$ as shown in the inset of Fig. 1. The curve labeled 2 $n_0$ takes into account a Gaussian absorption centered at 125 meV with a broadening multiplied by a factor 1.3 as observed on the S-P absorption. The curves have been offset and normalized for clarity. The inset shows the calculated intensity profile of the *z* component of the electric field at 100 meV over the 4 $\mu$m thickness.

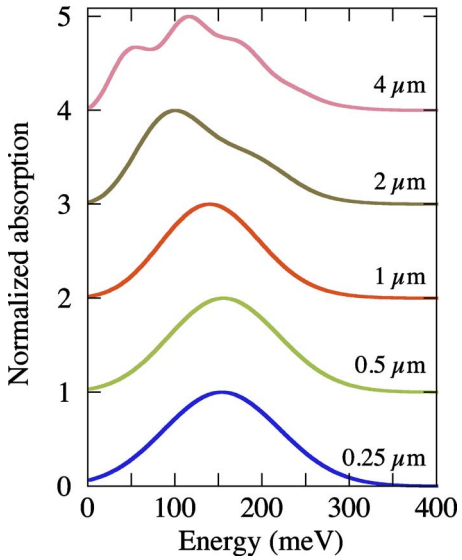


FIG. 4. (Color online) Influence of the quantum dot layer total thickness on the visibility of the interferences. The thicknesses of the active region (dots+GaAs barriers) are indicated on the graph. 4 $\mu$m thickness corresponds to 80 quantum dot layers separated by 50 nm. The absorption amplitude maxima have been normalized to unity. The curves have been offset for clarity. The effect of interference is clearly visible for thicknesses above 2 $\mu$m.

to-bound transitions like the S-D transitions might only be evidenced in absorption or photocurrent spectra once the standing wave patterns and interference effects are taken into account.

Another possibility to experimentally avoid the interferences is to perform the measurements in a slab waveguide geometry as done in Ref. 17 or to reduce the total thickness of the quantum dot layers. Figure 4 shows the effect of the quantum dot layer total thickness on the interference appearance. The curves have been normalized to unity and offset for clarity. Spectral modulations are clearly observed for thicknesses larger than 2 $\mu$m. This 2 $\mu$m threshold thickness obviously depends on the resonant wavelength of the bound-to-continuum intersublevel absorption as it is correlated with the periodicity of the intensity distribution. This spatial periodicity is given by $\lambda/[2n\cos(\alpha)]$ and is equal to 2.2 $\mu$m for 10 $\mu$m wavelength. As seen in Fig. 4, the interferences are not observed for thicknesses below 2 $\mu$m. The drawback of the thickness reduction is the decrease in absorption amplitude for a single pass. This effect can however be counterbalanced by an increase in the number of passes in the multipass geometry.

## V. CONCLUSION

We have shown that the measurement of quantum dot intersublevel absorption in the mid-infrared is influenced by three features. The quantum dot bound-to-continuum absorption is mainly $z$ polarized. Except for measurements on slab waveguides, the absorption is usually measured using a multipass geometry. The absorption amplitude of a single quantum dot layer is rather weak and the measurement of this absorption usually requires to stack a large number of layers, resulting in active region thicknesses of several micrometers. The quantum dot absorption is spectrally broad, thus increasing the probability to observe interferences on infrared absorption spectra which usually covers a large spectral range. The multipass geometry results in the formation of standing wave patterns with an intensity spatial periodicity which depends on the wavelength. Since the thickness of the quantum dot layers is usually of the same order of magnitude than the spatial periodicity of the light intensity, the integrated absorption over the total number of quantum dot layers is spectrally modulated. Consequently the standing wave pattern needs to be taken into account in order to interpret the absorption spectra. We have experimentally shown a good agreement between experimental absorption measurements and modeling for InGaAs quantum dot samples with various doping densities and two distinct incident angles. Three distinct approaches can lead to an unambiguous interpretation of the quantum dot absorption spectra: (i) an appropriate modeling of the standing wave pattern, as done in this work. (ii) A reduction in the number of quantum dot layers which can be compensated by an increase in the number of passes. (iii) The measurement of absorption using a slab waveguide geometry. In the latter case, it requires to embed the quantum dot layers into a thick dielectric slab waveguide.

[1] S. Sauvage, P. Boucaud, F. H. Julien, J. M. Gerard, and V. Thierry-Mieg, Appl. Phys. Lett. **71**, 2785 (1997).
[2] J. Phillips, K. Kamath, X. Zhou, N. Chervela, and P. Bhattacharya, Appl. Phys. Lett. **71**, 2079 (1997).
[3] H. Drexler, D. Leonard, W. Hansen, J. P. Kotthaus, and P. M. Petroff, Phys. Rev. Lett. **73**, 2252 (1994).
[4] S. Hameau, Y. Guldner, O. Verzelen, R. Ferreira, G. Bastard, J. Zeman, A. Lemaître, and J. M. Gérard, Phys. Rev. Lett. **83**, 4152 (1999).
[5] F. Bras, P. Boucaud, S. Sauvage, G. Fishman, and J. M. Gerard, Appl. Phys. Lett. **80**, 4620 (2002).
[6] K. W. Berryman, S. A. Lyon, and M. Segev, Appl. Phys. Lett. **70**, 1861 (1997).
[7] J. Phillips, K. Kamath, and P. Bhattacharya, Appl. Phys. Lett. **72**, 2020 (1998).
[8] S. Sauvage, P. Boucaud, T. Brunhes, V. Immer, E. Finkman, and J. M. Gerard, Appl. Phys. Lett. **78**, 2327 (2001).
[9] B. Aslan, H. C. Liu, M. Korkusinski, S.-J. Cheng, and P. Hawrylak, Appl. Phys. Lett. **82**, 630 (2003).
[10] H. Lim, W. Zhang, S. Tsao, T. Sills, J. Szafraniec, K. Mi, B. Movaghar, and M. Razeghi, Phys. Rev. B **72**, 085332 (2005).
[11] S. Sauvage, P. Boucaud, J. M. Gerard, and V. Thierry-Mieg, Phys. Rev. B **58**, 10562 (1998).
[12] S. Sauvage, P. Boucaud, F. H. Julien, J. M. Gerard, and J. Y. Marzin, J. Appl. Phys. **82**, 3396 (1997).
[13] J.-Z. Zhang and I. Galbraith, Appl. Phys. Lett. **85**, 5105 (2004).
[14] A. Schliwa, M. Winkelnkemper, and D. Bimberg, Phys. Rev. B **76**, 205324 (2007).
[15] G. A. Narvaez and A. Zunger, Phys. Rev. B **75**, 085306 (2007).
[16] P. Boucaud, S. Sauvage, and J. Houel, C. R. Phys. **9**, 840 (2008).
[17] P. Boucaud and S. Sauvage, C. R. Phys. **4**, 1133 (2003).
[18] S. Sauvage, P. Boucaud, T. Brunhes, F. Glotin, R. Prazeres, J. M. Ortega, and J. M. Gerard, Phys. Rev. B **63**, 113312 (2001).
[19] J. Houel, S. Sauvage, P. Boucaud, A. Dazzi, R. Prazeres, F. Glotin, J.-M. Ortega, A. Miard, and A. Lemaitre, Phys. Rev. Lett. **99**, 217404 (2007).
[20] W. H. Ng, E. A. Zibik, L. R. Wilson, M. S. Skolnick, J. W. Cockburn, and M. J. Steer, J. Appl. Phys. **103**, 066101 (2008).
[21] E. Zibik, A. Andreev, L. Wilson, M. Steer, R. Green, W. Ng, J. Cockburn, M. Skolnick, and M. Hopkinson, Physica E **26**, 105 (2005).
[22] L. R. C. Fonseca, J. L. Jimenez, J. P. Leburton, and R. M. Martin, Phys. Rev. B **57**, 4017 (1998).
[23] T. Grange, E. A. Zibik, R. Ferreira, G. Bastard, B. A. Carpenter, P. J. Phillips, D. Stehr, S. Winnerl, M. Helm, M. J. Steer, M. Hopkinson, M. S. Skolnick, and L. R. Wilson, New J. Phys. **9**, 259 (2007).
[24] A. M. Adawi, E. A. Zibik, L. R. Wilson, A. Lemaitre, J. W. Cockburn, M.

S. Skolnick, M. Hopkinson, and G. Hill, Appl. Phys. Lett. **83**, 602 (2003).
[25]M. J. Kane, M. T. Emeny, N. Apsley, C. R. Whitehouse, and D. Lee, Semicond. Sci. Technol. **3**, 722 (1988).
[26]J. Y. Andersson and G. Landgren, J. Appl. Phys. **64**, 4123 (1988).
[27]K. Vodopyanov, V. Chazapis, C. Phillips, B. Sung, and J. Harris, Semicond. Sci. Technol. **12**, 708 (1997).
[28]H. Schneider, C. Schonbein, M. Walther, P. Koidl, and G. Weimann, Appl. Phys. Lett. **74**, 16 (1999).